

## Long-Wavelength Transverse Modes in Charged Colloidal Crystals

B. V. R. Tata,<sup>1</sup> P. S. Mohanty,<sup>1</sup> M. C. Valsakumar,<sup>1</sup> and J. Yamanaka<sup>2</sup>

<sup>1</sup>*Materials Science Division, Indira Gandhi Centre for Atomic Research, Kalpakkam -603 102, Tamil Nadu, India*

<sup>2</sup>*Faculty of Pharmaceutical Sciences, Nagoya City University, 1-3 Tanabe-dori, Mizuho, Nagoya 467-8603, Japan*

(Received 6 April 2004; published 29 December 2004)

The dynamics of closely index matched colloidal crystals of charged silica spheres dispersed in deionized ethylene glycol-water mixture is investigated using dynamic light scattering. At variance with the reports of phonon dispersion measurements on thin colloidal crystals, our observations on millimeter-sized crystals show unambiguous evidence for overdamped transverse modes turning propagative in the range of small wave numbers in agreement with the theory of hydrodynamic interactions in charged colloidal crystals.

DOI: 10.1103/PhysRevLett.93.268303

PACS numbers: 82.70.Dd, 42.25.Fx, 63.20.-e

Submicron sized monodisperse charged colloidal particles dispersed in a deionized polar medium exhibit long-range order due to electrostatic interaction among the particles [1]. Such ordered dispersions are known as colloidal crystals (CCs) and exhibit body centered and face centered cubic (fcc) structures depending on the volume fraction  $\phi$ . CCs exhibit iridescence due to Bragg diffraction of visible light and their structure and dynamics can be investigated using static and dynamic light scattering techniques (DLS) [2–4]. These crystals differ from the atomic crystals not only in particle size and lattice constants but also in dynamics due to the hydrodynamic interaction that arises when moving colloidal particles exchange momentum through the intervening solvent [5]. The viscous solvent causes friction, which strongly dampens the lattice vibrations [2,4]. Theoretically, lattice dynamics has been treated in analogy with solid-state theory, the only modification being the incorporation of frictional forces. The theory of hydrodynamic interactions in charged CCs [2,4] predicts that the damping of transverse modes vanishes in the long-wavelength (i.e., wave number  $q = 0$ ) limit. All the other modes are predicted to be overdamped due to the strong frictional forces [2,4]. There is no relative motion of colloidal particles and the fluid at small wave numbers. Hence the overdamped transverse modes turn propagative, as  $q$  tends to zero [2,4]. So far, this prediction of hydrodynamic theory of charged CCs has not been observed experimentally and also the volume fraction dependence of this transition is not examined either theoretically or experimentally. However, shear modulus measurements have revealed the existence of propagating shear modes in CCs [6].

In this Letter we report the  $\phi$  dependence of this transition theoretically for charged CCs having bcc ordering and show experimentally, for the first time, overdamped transverse modes turning propagative in the range of small wave numbers in closely index matched colloidal crystals of charged silica particles dispersed in ethylene glycol-water (EGW) mixture. All previous experiments of phonon dispersion measurements in charged CCs were carried out

on dilute ( $\phi \approx 0.002$ – $0.005$ ) aqueous suspensions of polystyrene particles confined in a thin ( $\sim 30$ – $130 \mu\text{m}$ ) cell [2–4] to prevent multiple scattering of light. However, the transition of transverse modes turning from overdamped to propagative was not observed in these measurements. This discrepancy between the theory and experiment was attributed to the effect of walls that are concomitant with the thin cell geometry [2–4]. We have been successful in growing millimeter-sized charged CCs of silica particles dispersed in EGW (90:10) mixture. These CCs are free from multiple scattering due to close matching of refractive index of the particles with that of the medium and are also free from the wall effects due to the large ( $\sim 3 \text{ mm}$ ) size. Our DLS experiments on these crystals show a peak in the small  $q$  regime providing evidence for the transition in agreement with the theoretical prediction.

Existing lattice dynamics calculations [2–4], which incorporate harmonic potentials up to the second nearest neighbor distance and hydrodynamic interactions to the lowest order in  $\phi$ , suffice to describe the dynamics of dilute charged CCs. We have carried out lattice dynamics calculations by considering harmonic interactions with *all* the neighbors and hydrodynamic interactions for arbitrary  $\phi$  using appropriate Ewald summation techniques [7]. The charged spheres are assumed to interact via screened Coulomb potential  $U(r) = [eZe^{\kappa a}/(1 + \kappa a)]^2 \exp(-\kappa r)/\epsilon r$  [1,2], where  $a$  ( $= 53 \text{ nm}$ ) and  $Ze$  ( $= 500e$ ) are the radius and effective charge on the particle, respectively,  $\epsilon$  ( $= 78$ ) is the dielectric constant of the medium, and the inverse Debye screening length  $\kappa$  is given by  $\kappa^2 = (4\pi e^2/\epsilon k_B T)(n_p Z + C)$ . Here  $C$  is the salt concentration,  $T$  is the temperature ( $300^\circ \text{K}$ ),  $k_B$  is the Boltzmann constant, and  $n_p$  ( $= 3\phi/4\pi a^3$ ) is the particle concentration. Figure 1 shows the volume fraction dependence of dispersion curves of longitudinal and transverse modes for a bcc lattice along [110] direction. Dispersion of longitudinal modes for low values of  $\phi$  is in qualitative agreement with that observed in experiments on dilute colloidal crystals confined in thin cells [2–4]. The decay rate

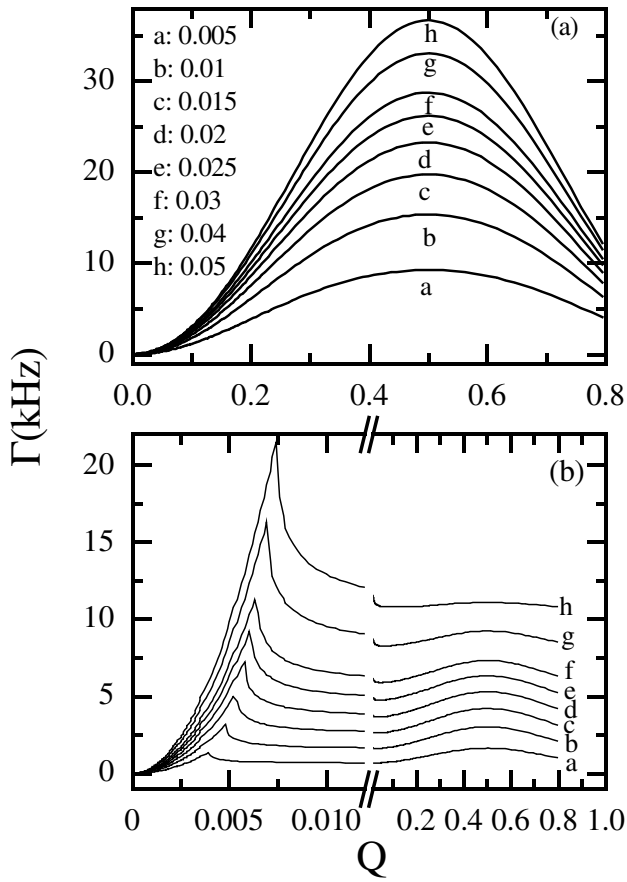


FIG. 1. Theoretical phonon dispersion curves for a bcc colloidal crystal as a function of the reduced wave number  $Q$  in the  $[110]$  direction for different values of  $\phi$ . (a) Longitudinal mode. (b) Transverse mode. The lattice dynamics theory with hydrodynamic friction predicts transition of overdamped mode to propagative in the low  $Q$  regime, and the sharp peak in (b) is due to this transition.

$\Gamma (= \omega_q^2 / \lambda_q)$ , where  $\omega_q$  represents the undamped frequency of the oscillator and  $\lambda_q$  represents the corresponding friction factor) of longitudinal modes as a function of  $Q$ , where  $Q = qR_0 / (2\sqrt{2}\pi)$  is the reduced wave number and  $R_0$  is the lattice constant, increases as a function of  $\phi$  due to mode hardening of the undamped lattice. The  $\phi$  dependence of transverse modes [Fig. 1(b)] at large  $Q$  is similar to that of the longitudinal mode. However, in the small  $Q$  regime, it exhibits a sharp peak [8] that represents the transition of overdamped transverse mode into a propagative mode. Though Hoppenbrouwers and van de Water's calculations [4] predicted this transition to occur at  $Q \approx 0.0027$  for a sample with  $\phi = 0.0025$ , they failed to observe it because of the use of CCs confined in a thin cell. Our calculations have shown that the two transverse modes in  $[110]$  direction are nondegenerate. Both modes are predicted to show a transition from overdamped to propagative in the low  $Q$  regime. The first mode that is accessible to our experiment is shown in Fig. 1(b). The

second mode has a weaker  $\phi$  dependence and the transition should occur around  $Q \approx 0.001$ . Further, its decay rate is 1 order of magnitude smaller compared to the first mode and hence the transition is undetectable in our experiment. It will not therefore be discussed further in this Letter.

It is clear from Fig. 1(b) that the peak shifts to higher value of  $Q$  as  $\phi$  increases, hence CCs of large  $\phi$  are more suitable for observing the peak in dynamic light scattering experiments provided the multiple scattering of light is suppressed. In CCs, multiple scattering can be suppressed by matching closely the refractive index of the particle  $\mu_p$  with that of the host fluid  $\mu_m$ . We achieve this in a charged colloidal system consisting of silica particles having a radius of  $60 \pm 5$  nm by redispersing [9] the aqueous silica suspension in pure ethylene glycol. Mother suspension with 90:10 EGW mixtures was left for complete deionization after adding a known amount of mixed-bed of anion and cation exchange resin beads (AG 501 X8 (D), Biorad, USA). Effective surface charge number  $Z$  on the silica particles, determined from conductivity measurements, is  $\sim 410 \pm 65$  [10] and the residual salt concentration in the suspension  $C \sim 1 \mu\text{M}$ . The refractive index difference  $\Delta\mu$  between particle and the 90:10 EGW medium is only 0.04, and is 6.5 times smaller than that compared to the aqueous suspension of polystyrene particles. Hence the silica-EGW system is free from multiple scattering. The absence of significant scattered intensity from our CCs in the depolarized geometry also confirms the absence of multiple scattering. This allowed us to carry out light scattering studies over a wide range of volume fractions ( $\phi \sim 0.0006$ – $0.12$ ) [9]. We report here the DLS measurements carried out at room temperature on two samples S1 and S2 having volume fractions 0.048 and 0.064, respectively.

Deionized suspensions were introduced in 8 mm optical path length cylindrical quartz cells. For further removal of ionic impurities, clean nylon net bags containing the mixed-ion exchange resins were hung from the top of the cell and sealed hermetically. After about seven days, the sample showed iridescence with crystallites having a mean size of  $\sim 3$  nm (inset of Fig. 2). Our light scattering system consists of a (Ar + Kr) mixed-ion laser and a 50 mw He-Ne laser, Malvern (UK) 4700 multitaum correlator and a goniometer, with photomultiplier tube as the detector. The axis of the sample cell is along the  $z$  direction and scattering plane is the horizontal  $xy$  plane. The sample cell is placed in a cylindrical vat containing refractive index matching fluid (water) that also serves as a temperature bath. We have made provision to rotate the sample cell around the vertical axis ( $z$  axis) and adjust the cell height.

The normalized electric field autocorrelation  $g^{(1)}(k, t)$ , obtained from the measured scattered-light correlation function  $g^{(2)}(k, t)$  using Siegert relation [2,3,9], is related to the time autocorrelation function  $\rho_q^\nu(t)$  of the normal modes  $K_q^\nu(t)$  [4,5,11] of CCs by

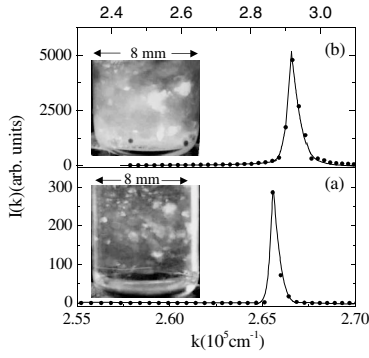


FIG. 2. Scattered intensity  $I(k)$  versus  $k$  from crystallites at the center of the cell, whose (110) planes are oriented perpendicular to the scattering plane ( $xy$  plane). (a) In sample S1, (110) Bragg peak occurs at  $k = 2.656 \times 10^5 \text{ cm}^{-1}$ . (b) In sample S2 Bragg peak occurs at  $k = 2.918 \times 10^5 \text{ cm}^{-1}$ . The corresponding lattice constants of samples S1 and S2 are  $R_0 = 0.335$  and  $0.302 \text{ } \mu\text{m}$ , respectively.  $R_0$  is calculated using the relations  $R_0 = 2\sqrt{2}\pi/k_{110}$  and  $R_0 = d(\pi/3\phi)^{1/3}$ . Both gave the same value. The insets show photographs of samples S1 and S2 having large size (about 3 mm) single crystals exhibiting iridescence under white light illumination.

$$g^{(1)}(\vec{k}, t) = \frac{8\pi^3}{\Omega} e^{-2M} \sum_m \delta^3(\vec{k} - \vec{k}_m) + \sum_{q, \alpha, \nu} (k^\alpha n_q^{\alpha\nu})^2 \times \langle |\vec{K}_q^\nu|^2 \left[ \frac{8\pi^3}{\Omega} \sum_m \delta^3(\vec{k} - (\vec{k}_m - \vec{q})) \rho_q^\nu(t) \right] \rangle + \dots,$$

where  $\vec{q}$  is the wave vector of the phonon,  $\alpha$  the coordinate label,  $\nu$  polarization,  $n_q^{\alpha\nu}$  the amplitude,  $\Omega$  the volume of direct-lattice unit cell, and  $M$  is the Debye-Waller exponent. The first term represents zero-phonon scattering (Bragg scattering) that occurs when the scattering wave vector  $\vec{k}$  equals a reciprocal lattice vector  $\vec{k}_m$ . The second term corresponds to one-phonon scattering, which is quasi-elastic. In CCs, all but the long-wavelength transverse modes are overdamped, hence  $\rho_q^\nu(t)$  decays exponentially as  $\rho_q^\nu = \exp(-\Gamma_q^\nu t)$ , with  $\Gamma_q^\nu = (\omega_q^\nu)^2 / \lambda_q^\nu$ . The wave vector  $q$  of the phonon can be selected experimentally as the difference between  $\vec{k}$  and the nearest reciprocal lattice vector  $\vec{k}_m$ . The scattering geometry in our experiments is such that for a given  $\vec{k} = \vec{k}_m + \vec{q}$ , only the longitudinal and transverse phonons of wave vector  $q$  contribute to  $g^{(1)}(k, t)$ .

Charged CCs having a bcc structure are known to grow with their closest packed plane parallel to the cell wall [2–4]. We pick up the sharply defined (110) Bragg reflection (Fig. 2) in the scattering plane from the crystallites in our samples S1 and S2 by adjusting the cell orientation. Bragg angle corresponds to the setting with phonon wave vector  $q = 0$ . We have studied longitudinal and transverse mode dispersion along [110] direction by rotating the detector by angle  $2\theta$  starting from Bragg angle and rotating the cell by

angle  $\theta$ . The decay rates  $\Gamma$  of longitudinal and transverse modes are obtained by subjecting  $g^{(1)}(k, t)$  to mixed mode analysis using nonlinear-least square fit method [2–4].

Figure 3 shows the measured phonon dispersion curves in the first and second Brillouin zone along the [110] direction. The dispersion curves of the longitudinal mode [Fig. 3(a)] are similar to those observed in thin cells and the  $\phi$  dependence is in qualitative agreement with our lattice dynamics calculations discussed in Fig. 1(a). The measured transverse modes, apart from exhibiting the expected dispersion away from small  $Q$  regime also show a sharp peak at  $Q \approx 0.076$  in a crystal with  $\phi = 0.048$  and at  $Q \approx 0.11$  in a crystal with  $\phi = 0.064$ . The observation of sharp peaks constitutes an unambiguous evidence for the transition of the overdamped transverse modes to propagating modes as predicted by the hydrodynamic theory of charged CCs. The observation that the peak shifts from 0.076 to 0.11 with increase in  $\phi$  is also in qualitative agreement with our lattice dynamics calculations presented in Fig. 1(b). Though there is a qualitative agreement between Fig. 1 and Fig. 3, there exist noticeable differences. (a) The dispersion relation in Fig. 1, which is obtained using harmonic theory of lattice vibrations, passes through the origin both for longitudinal and transverse mode whereas it does not in Fig. 3. Previous measurements [4,11] of dispersion curves on polystyrene colloids also report  $\Gamma(0) \neq 0$  at  $Q = 0$ . It is well known in the context of atomic systems that *static disorder* and *anharmonicity* cause broadening (increase of linewidth) of phonon peaks [12,13]. The *static disorder* in our CCs arises due to  $\sim 8\%$  size polydispersity (SPD) which in turn leads to charge polydispersity (CPD) [1,14]. The SPD of 8% that

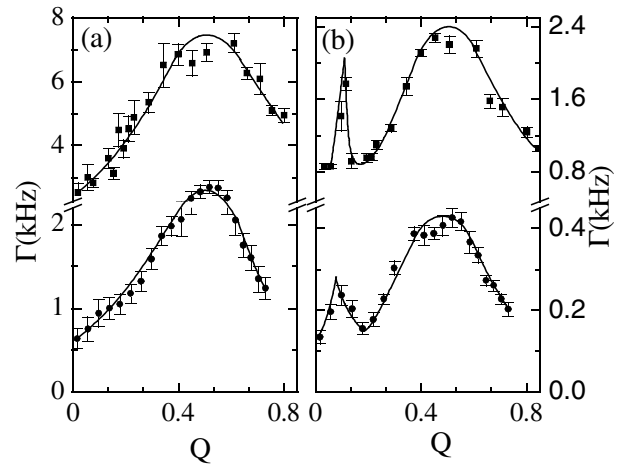


FIG. 3. Measured phonon dispersion curves along 110 direction of colloidal single crystals of 3 mm size and having bcc structure. (a) Longitudinal. (b) Transverse. Filled circles and filled squares correspond to dispersion in crystals with  $\phi = 0.048$  and  $0.064$ . The lines are guides to the eye. Note that the transverse mode turns propagative at  $Q \approx 0.076$  in a crystal with  $\phi = 0.048$  and at  $Q \approx 0.11$  in a crystal with  $\phi = 0.064$ .

is present in our silica colloidal crystals is higher as compared to the SPD of  $\sim 1.3\%$  of polystyrene particles used in earlier experiments [4]. Hence  $\Gamma(0)$  in our case is expected to be larger than that reported in earlier experiments [4,11]. There is also evidence for strong *anharmonicity* in charged CCs (Lindemann parameter  $W > 0.17$ ) [1,14]. The CCs reported in the present work are not close to melting transition. However, we have estimated  $W$  [9] from DLS measurements for our samples and it is found to be  $W \sim 0.13$ . This number is larger than that in atomic crystals at melting and hence our crystals are expected to have strong anharmonicity. (b) Peak positions and peak heights are also found to differ in Figs. 1 and 3. It is known from the studies in atomic systems that anharmonicity can lead to a shift in phonon frequencies in addition to increase in the linewidth [13]. Our calculations within the harmonic theory have shown a strong dependence of peak height and peak position on  $Ze$  [10]. Further, the resolution  $\delta Q$  with which we locate the peak near zone center in the case of Fig. 1 is about 2 orders of magnitude higher than in the experiment ( $\delta Q = 0.025$ ). Hence we attribute the difference between theory (Fig. 1) and experiment (Fig. 3) to anharmonicity, to the low resolution in  $Q$ , etc. Thus, we conclude that even though there is a qualitative agreement between theory and experiment, the theory in its present form is not comprehensive enough to provide a quantitative interpretation in the entire  $Q$  regime. Our observations also support the view that finite thickness [2,15] is responsible for observing the relaxation rate of transverse modes  $\Gamma \rightarrow 0$  as  $q \rightarrow 0$  in CCs confined in thin cells rather than ion retardation effects [16].

In conclusion, we have grown multiple scattering free millimeter-sized charged silica CCs in EGW medium and observed for the first time a sharp peak close to Brillouin zone center. This observation confirms the theoretical prediction that overdamped transverse modes in charged CCs turn propagative in the long-wavelength limit. It is interesting to note that Stark and Trebin [17] obtain a similar dispersion curve for the displacement modes of the blue phase of liquid crystals in the low  $Q$  regime without the hydrodynamic interaction. Our experiments point out the need for a hydrodynamic theory of CCs with polydispersity and anharmonicity. We believe that the present work paves the way further theoretical and experimental studies on dynamics in colloidal alloys and CCs of highly charged particles, where counterion dynamics might play some role in influencing the dynamics.

---

[1] B. V. R. Tata, *Curr. Sci.* **80**, 948 (2001); A. K. Arora and B. V. R. Tata, *Adv. Colloid Interface Sci.* **78**, 49 (1998).

- [2] A. J. Hurd, N. A. Clark, R. C. Mockler, and W. J. O'Sullivan, *Phys. Rev. A* **26**, 2869 (1982).
- [3] J. Derksen and W. van de Water, *Phys. Rev. A* **45**, 5660 (1992).
- [4] M. Hoppenbrouwers and W. van de Water, *Phys. Rev. Lett.* **80**, 3871 (1998); M. Hoppenbrouwers, Ph. D. thesis, Eindhoven University of Technology, 1998.
- [5] H. Hasimoto, *J. Fluid Mech.* **5**, 317 (1959).
- [6] T. Palberg *et al.*, *J. Phys. III (France)* **4**, 457 (1994).
- [7] M. C. Valsakumar and B. V. R. Tata (to be published).
- [8] The physics behind the occurrence of a peak at small  $Q$  in the dispersion curves of transverse modes is as follows. The relative motion between the particles and the fluid almost vanishes for the transverse modes as  $q \rightarrow 0$  and the effective friction coefficient  $\lambda_T(q, \omega)$  of both the transverse modes vary quadratically with  $q$  for small  $q$  [2]. In this limit, the amplitude  $u_q$  of the modes approximately satisfy the damped harmonic oscillator equation  $\mu(d^2u_q/dt^2) + m_F v_q(du_q/dt) + m_p \Omega_q^2 u_q = 0$ , where  $\mu = m_p + m_F$ ,  $m_p$  is the mass of the particle,  $m_F$  is the mass of the fluid in a unit cell,  $v_q = \eta q^2 / \rho$ ,  $\Omega_q = cq$ , and  $c$  is the velocity of the shear sound. It is easily seen that the modes are underdamped for  $q < q_*$  ( $2\rho c \sqrt{\mu m_p} / \eta m_F$ ). In this regime, the decay rate  $\Gamma$  of  $u_q(|u_q| \sim e^{-\Gamma t})$  is given by  $\Gamma = v_q m_F / 2\mu$  which increases quadratically with  $q$  until  $q_*$ . For  $q > q_*$ , the motion is overdamped and the smallest decay rate is given by  $\Gamma = (\tilde{v}_q/2) - \sqrt{(\tilde{v}_q^2/4) - \tilde{\Omega}_q^2}$  (where  $\tilde{v}_q = v_q m_F / \mu$  and  $\tilde{\Omega}_q^2 = \Omega_q^2 m_p / \mu$ ), which decreases as  $q$  increases. Thus the decay rate  $\Gamma$  has a peak at  $q_*$ . We believe this peak arises due to approximate matching of time scales associated with the frictional and restoring forces. When  $\tilde{v}_q \sim 2\tilde{\Omega}_q$ , the energy transfer from the particle to the fluid occurs most efficiently, leading to faster decay.
- [9] B. V. R. Tata, P. S. Mohanty, J. Yamanaka, and T. Kawakami, *Mol. Simul.* **30**, 153 (2004).
- [10] Effective charge  $Ze$  measured by conductivity method is estimated from the slope of the plot of conductivity versus  $\phi$  [1] and also by shear modulus measurements [Wette *et al.*, *J. Chem. Phys.* **116**, 10981 (2002)] on CCs. The value of  $Ze$  value estimated from the shear modulus measurements is found to be 40% smaller than that obtained by conductivity method.
- [11] Z. Cheng, J. Zhu, W. Russel, and P. M. Chaikin, *Phys. Rev. Lett.* **85**, 1460 (2000).
- [12] G. Ruocco *et al.*, *Phys. Rev. B* **54**, 14892 (1996); P. Johansson, *Phys. Rev. B* **54**, 2988 (1996).
- [13] N. M. Gasanly, *Cryst. Res. Technol.* **38**, 962 (2003); T. R. Ravindran and A. K. Arora, *Phys. Rev. B* **67**, 064301 (2003).
- [14] H. Löwen, *Phys. Rep.* **237**, 249 (1994).
- [15] P. P. J. M. Schram, A. G. Sitenko, and V. I. Zasenkov, *Physica B (Amsterdam)* **228**, 197 (1996).
- [16] B. U. Felderhof and R. B. Jones, *Faraday Discuss. Chem. Soc.* **83**, 69 (1987).
- [17] H. Stark and H. R. Trebin, *Phys. Rev. E* **51**, 2326 (1995).